Weldability Improvement Using Coated Electrodes for RSW of HDG Steel

K. R. Chan, N. Scotchmer
Huys Industries Limited, 175 Toryork Drive Unit #35, Weston Ontario, M9L 1X9, Canada

J. Zhao, Y. Zhou.
University of Waterloo, 200 University Avenue West Waterloo, Ontario, Canada N2L 3G1

ABSTRACT

The increased use of zinc coatings on steels has led to a decrease in their weldability. Weld current and time need to be increased in order to achieve sound welds on these materials compared to uncoated steels, and electrode tip life suffers greatly due to rapid alloying and degradation. In this work, typical uncoated Class II electrodes were tested along with a TiC metal matrix composite (MMC) coated electrode. Tests were conducted to study the weldability and process of nugget formation for both electrodes on HDG (hot dipped galvanized) HSLA (high strength low alloys) steels. Current and time ranges were constructed for both types of electrodes by varying either the weld current or weld time while holding all other parameters constant. Analysis of weld microstructures was conducted on cross-sectioned welds using SEM (scanning electron microscopy). Using the coated electrodes reduced weld current and times needed to form MWS (minimum weld size) on the coated steels. Current and time ranges forming satisfactory nuggets were also increased, improving the weldability of the steels. A notable cooling effect was found at the EW (electrode workpiece) interface of the steel sheet and was confirmed by software modeling to be due to rapid cooling through the electrode. The coated electrode weld did not exhibit the cooling artifact, which was believed to be due to the thermal effects of the TiC MMC coating.

 The lower weld current and time needed to form welds of MWS when using the coated electrodes as well as the increase in the usable current and time range indicate an increase in the weldability of the coated electrodes when welding HDG material. This notable improvement was caused by the presence of the TiC MMC electrode coating increasing the interfacial resistance as well as acting as a thermal barrier preventing the rapid extraction of heat from the faying interface through the electrodes leading to larger weld sizes at identical weld parameters than the uncoated electrodes.

INTRODUCTION

Resistance spot welding (RSW) remains to be a heavily used method for joining sheet steel components in the automotive industry. The use of zinc coated steels has increased significantly over the past decade, owing to their good corrosion resistance and relatively low cost. The zinc coating present on the steel surface has increased the difficulty of welding due to its lower electrical resistance and melting temperature [1]. This has led to the use of higher welding currents and times in order to weld the coated steels, resulting in higher costs and reduced tip life. The poor weldability requires the use of more frequent current stepping and/or tip dressing to maintain weld quality and incurs higher costs. These issues are of great concern for automotive manufacturers.

Electrode degradation during resistance welding of coated steels has been the subject of many studies [2-13]. Developments in electrode materials and design have been explored by other researchers in an effort to increase the weldability of coated steels and electrode life with mixed results.

Previous unpublished work has shown that TiC MMC coated electrodes were able to yield approximately double the tip life of traditional uncoated Class II CCZ electrodes. This study concluded that the main function of the TiC MMC electrode coating was to protect the copper base material of the electrode from interaction and alloying with the zinc from the steel coating. The weld current and time windows of the coated electrode were also noted to be shifted lower and wider than those

of the uncoated electrode. The increased weldability of coated steels when using these coated electrodes was thought to be due to the thermal interaction effects that the electrode coating had with the steels during the weld.

In the present work, the effects of the TiC MMC electrode coating on the formation and final shape of the weld nugget when welding hot-dip galvanized steels were studied. Weld simulations were conducted with the modelling software SORPAS® to assist in understanding of the development of the nugget and heat flow. Weldability windows for weld current and time were also constructed for uncoated electrodes as well as the coated electrodes. This study is aimed at understanding the thermal effects of the coated electrode on the formation and development of the weld nugget by weld testing and simulation.

TECHNICAL BACKGROUND

The weld nugget in RSW is formed by the passing of current through the electrodes and the worksheets. Heat is generated due to the passing of current by the contact resistances at the interfaces and bulk resistances in the workpieces governed by the equation $H=I^2Rt,$ where H is the total heat, I the weld current, R the total circuit resistance, and t the weld time. H represents the total amount of heat input to the system, however the quality of the weld formed is directly dependant on the localized heat generation, or $H/A,$ where A is the area of the contact face of the electrode. This is in turn influenced by I/A known as current density.

The presence of the low resistance zinc coating at the faying interface requires a higher welding current to be used to form satisfactory weld nuggets. The sheet coating changes the process of nugget formation compared to uncoated steels and can have adverse effects on the electrode wear character as well [12,16,17]. The resistances at all the interfaces are very similar and so heat generation is also similar at each interface. This causes much more heat to be generated at the electrode-sheet interfaces than with uncoated steels [18,19]. The good thermal conductivity of the copper alloy electrodes assisted by active water cooling provide enough heat sinking to restrict the weld nugget to the faying interface. This leads to narrow weldability lobes and poor system reliability. Observing the heat generation and dissipation as the weld progresses is very difficult as the weld is formed internally between the worksheets and is not accessible by traditional sensing equipment. The ability to model the spot weld as it is being formed has been achieved by resistance spot welding simulation software. The software is able to predict weld nugget growth by combining factors involved in the thermal, mechanical, electrical and metallurgical models of welding.

Weld current range (WCR) is defined as the range of weld current varied while holding all other weld parameters constant which yield satisfactory welds.

Weld current is taken as the root mean squared (RMS) value of welding current required to form welds that meet the upper and lower bounds of allowable weld quality. The upper and lower bounds of the weld current range that define satisfactory nuggets are commonly set to the physical expulsion limit and minimum weld size criteria of $3.5\sqrt{t}$ or $4\sqrt{t}$ respectively, where t is the governing material thickness of the sheets being welded. The larger the WCR for the system of electrodes and worksheets, the greater the reliability of the system becomes.

The following investigations were performed to observe how the coated electrode nugget formation sequence differed from that of the uncoated electrode. Simulations were conducted using resistance welding modelling software to generate current and time ranges for the coated and uncoated electrodes. Heat generation and propagation was observed and then compared to actual weld samples at selected weld parameters.

2 EXPERIMENTAL SETUP

2.1 SIMULATION OF WELDS

Simulations were conducted using SORPAS® *Version 6.0 Enterprise Edition* (*Copyright © 2005 SWANTEC Software and Engineering ApS*)[20] resistance weld simulation software. Welding parameters were input identical to those used in laboratory trials. The software is able to incorporate the mechanical and electrical model of resistance welding with the thermal heat flow model and metallurgical properties of the materials involved in the entire welding system. This results in a finite element model that very closely mimics the actual welding process. Output data from the simulations include maximum nugget diameter, molten nugget volume by time, stress and strain mappings, cooling rate, and temperature profiles. The simulation is able to be stopped at any time in the weld schedule to view the weld in process. Simulation parameters for material properties and interfacial properties were taken from the SORPAS® material databases provided with the software.

2.2 LABORATORY TESTING

Welds were made on hot-dip galvanized low carbon HSLA steel (HDG-70) 1.0mm and (0.0394in) thick with a UTS of 375 MPa (54ksi). Material preparation and welding were carried out as per AWS D8.9-97 [21]. Test pieces were cut to 38.5cm x 6cm (15.16 x 2.36 in) for life test coupons and 10cm x 3cm (3.6 x 1.18 in) for peel coupons. Welding was performed on a 250kVA, air operated, pedestal type, single-phase AC spot welding machine using RWMA Class 2 (Cu-Cr-Zr) domed-flat type (B-nose) female electrodes. Figure 1 shows a schematic sectional drawing of the electrode shape [15]. The TiC coated electrodes used in this study were identical in geometry and composition to the uncoated

electrode except for the addition of the TiC metal matrix composite approximately 20-40μm in thickness on the electrode face surface. The coating covers the flat area as well as the surrounding domed area of the electrode face. The TiC coating composition is shown in Table 1.

The coated matrix is composed mainly of Ni with some Mo, W and Cu introduced from the electrode base material mixing [14]. The Ti shown in Table 1 is in the form of TiC ceramic particles held in the metal matrix. The coating material in the form of a sintered rod was applied to the surface of the electrode using electro-spark deposition. Measured hardness (HV_{200}) of the coating rod, coated layer, and base electrode were found to be 2250, 980, and 174 respectively [14].
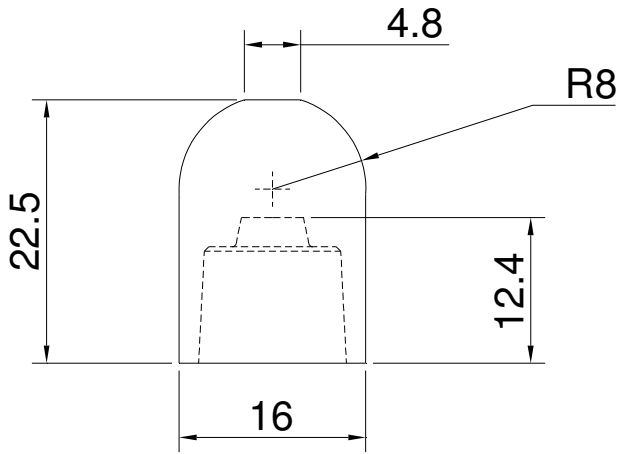

Figure 1: FB-25 Electrode Schematic Diagram. All dimensions in mm. (1mm = 0.039in)

	Ti	Ni	Mo	W	Cu
TiC Coated Layer	59.3	22.4	13.13	1.02	4.14

Table 1: Coated Electrode Coating Composition as measured by EDS

The welding schedules for both electrodes are given in Table 2. Weld parameters were taken from the suggested practice of tip life tests given by the AWS D8.9-97 [21]. Weld currents for each electrode were determined as the expulsion current minus 200A specified in the AWS. Welding currents used yielded an initial button size of 5mm ($6\sqrt{t}$). No cleaning of the electrode face was performed prior to welding. The HDG

steel sheets were hand wiped with paper towel prior to welding to remove excess mill oils and loose debris.

Steel Type	Electrode Type	Welding current (A)	Electrode force (lbf)	Weld time (cycle)	Hold time (cycle)	Welding rate (welds/min)	Cooling water
1.0mm Steel	Uncoated electrode	various	670	various	5	25	2
	Coated electrode	various	670	various	5	25	2
0.7mm Steel	Uncoated electrode	various	445	various	5	25	2
	Coated electrode	various	445	various	5	25	2

Table 2: Welding Schedules determined by AWS Standards [21] for Testing Electrodes

Weld peel button size was used as an indication of weld nugget size and was determined by peel testing (Figure 2) of weld samples and measurement of the pulled-out button. Cross sections of the welds were observed by optical microscopy.
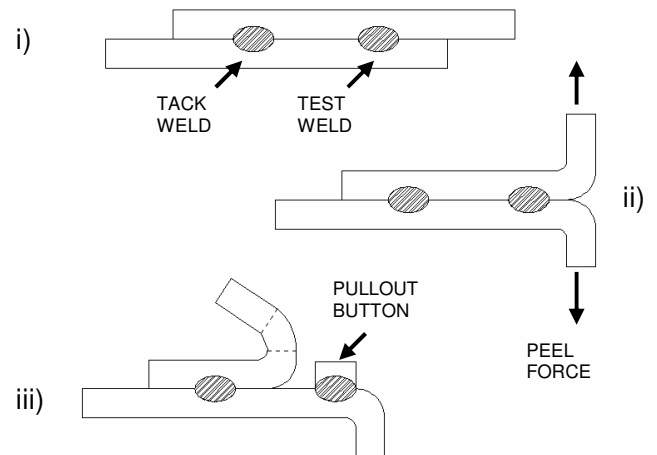

Figure 2: Peel Test Schematic

3 RESULTS

3.1 WELD CURRENT STUDY

Weld current ranges were determined for both coated and uncoated electrodes. Weld time was held at 13 cycles (217ms) for both electrode types and weld current was increased at 200A intervals until interfacial fusion, MWS, and expulsion conditions were reached. Simulations of the welds were also performed at the same weld current intervals which yielded predicted weld nugget sizes. Table 3 show the actual and predicted current tests results for both electrode types. For both actual and predicted weld sizes, the coated electrode was able to cause fusion of the sheets, and reach the minimum weld size at a lower current than the uncoated electrode. The ability of the coated electrode to form acceptable welds at lower currents indicated its improved weldability over the uncoated electrode. The increased range of weld current over which the coated electrode was able to form welds was also indicative of its superior weldability. The usable weld current range was 1400A for the coated electrode in weld trials, compared to the 800A for the uncoated electrode. As the simulation was not able to predict expulsion, expulsion was assumed to have occurred when the nugget size reached 6.5mm. Predicted current ranges were then 2600A and 1600A for the coated and uncoated electrodes respectively. Although the predicted values are slightly larger than the actual values found by welding trials, the trend of the coated electrode having a larger current range as well as forming MWS at lower current remains common.

Weld Current at 13 Cycles (A)	Welding Trial Button Size / Joint Condition		Simulation Results Button Size / Joint Condition	
	Coated Electrode	Uncoated Electrode	Coated Electrode	Uncoated Electrode
8800	0	0	0	0
9000	0	0	2.6	0
9200	0	0	3.6	0
9400	Interfacial Failure	0	4.1 (MWS)	0
9600	3.1	0	4.5	0
9800	4.2 (MWS)	0	4.7	0
10000	4.84	0	4.9	2.9
10200	5.6	Interfacial Failure	5.1	4.1 (MWS)
10400	5.8	3.6	5.49	4.4
10600	6.16	4.5 (MWS)	5.55	4.9
10800	6.2	5.57	5.8	5.3
11000	6.4	5.8	5.9	5.6
11200	6.5 (Expulsion)	6.3	6.1	5.8
11400	6.45 (Expulsion)		6.25	6.1
11600			6.4	6.2
11800			6.43	6.5
12000			6.5	6.7

Table 3: Weld Current Test Results at 13 cycle Weld Time on 1.0mm Steel

3.2 WELD TIME STUDY

It was seen in previous trials that the coated electrodes would require less weld current to produce satisfactory nuggets. In an effort to determine if the processes for nugget formation were different for coated and uncoated electrodes, weld time was set to terminate the weld current before the completion of the weld sequence to freeze the weld at each cycle of the sequence. Table 4 shows the weld time required to achieve fusion of the steel, form a weld that meets minimum weld size, and cause expulsion while holding weld current at 10500A. Simulation of the weld at 10500A was also conducted and produced graphs of the melted volume of steel for both uncoated and coated electrode situations shown in Figures 3 and 4. Both electrodes under the same weld schedule were also observed to have melted the zinc coating at the faying interface after 2 cycles (33ms) of weld current. The large difference in character was the number of cycles required to achieve fusion of the worksheets. Almost double the weld time was required for the uncoated electrode at 13 cycles (217ms) compared to the 7 cycles (117ms) for the coated electrode. Predicted melting time for the base metals was estimated for a melted volume above 4mm^3 to account for the molten zinc volume. Predicted time was approximately 200 and 140ms for uncoated and coated electrodes. Both predicted and welding results show that the uncoated electrode required longer welding times to achieve the same nugget size as the coated electrode under identical welding parameters.

Minimum weld sizes were achieved at 10 and 14 cycles (167 and 233ms) for the coated and uncoated electrodes respectively. Expulsion occurred at 15 and 17 cycles (250 and 283ms) for the coated and uncoated electrodes respectively. The number of weld current cycles between the fusion point and the expulsion point can give an indication of the weldability of the electrode. The coated electrode was able to form welds between 7 and 15 cycles (117 and 250ms) yielding an 8 cycle (133ms) range. The uncoated electrode time range was only from 13 to 17 cycles (217 to 283ms), half that of the coated electrode.

Weld Time		Button Size / Joint Condition	
(ms)	(cycles)	Coated Electrode	Uncoated Electrode

Weld Time (ms)	cycles	Uncoated Electrode	Coated Electrode
17	1	0	0
33	2	0	0
50	3	0	0
67	4	0	0
83	5	0	0
100	6	0	0
117	7	Interfacial Failure	0
133	8	3.46	0
150	9	3.74	0
167	10	4.7 (MWS)	0
183	11	5.09	0
200	12	5.2	0
217	13	5.6	Interfacial Failure
233	14	6.15	4 (MWS)
250	15	6.53 (Expulsion)	5.2
267	16		6.46
283	17		6.6 (Expulsion)

Table 4:   Weld Time Test Results at 10500A Weld Current

Weld Time (ms)	cycles	Uncoated Electrode	Coated Electrode
33	2	0.00	0.00
50	3	0.00	0.00
67	4	0.00	0.00
83	5	0.00	0.00
100	6	0.00	0.00
117	7	2.41	1.00
133	8	3.80	3.08
150	9	4.11	4.02
167	10	4.55	4.50
183	11	5.25	5.20
200	12	5.28	5.14
217	13	5.52	5.48
233	14	Expulsion	5.61
250	15	Expulsion	5.56
267	16	Expulsion	Expulsion

Table 5:   Weld Time Test Results for 0.7mm steel

A similar study conducted previously on 0.7mm HDG steel also shows the trend of the coated electrode being able to form nuggets sooner than a traditional uncoated electrode [24]. Table 5 shows the development of a weld nugget as weld time is increased in increments of one cycle while other weld parameters are held constant. The nominal weld size of 4.5mm was reached at 10 cycles for both coated and uncoated electrodes; however the weld currents for both electrodes were not the same. The weld current was set at 9200A for the uncoated electrodes while the coated electrode weld current was set at 8500A. These weld currents were established by finding the current windows at 10 cycles of weld time. It is clear that the coated electrode requires less heat input to form the same size weld. The expulsion limit shown in Table 5 also shows the coated electrode to be able to form welds up to 15 cycles of weld time at the 8500A, whereas the uncoated electrode is limited to 13 cycles before the onset of expulsion.
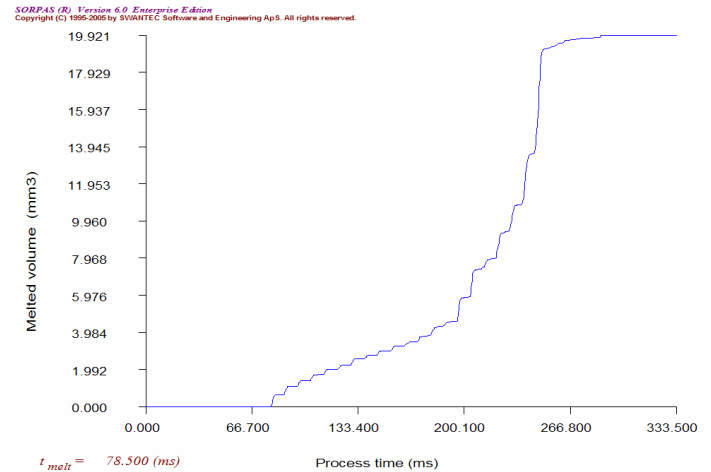

Figure 3: Predicted melted volume of metal for uncoated electrode weld at 10500A

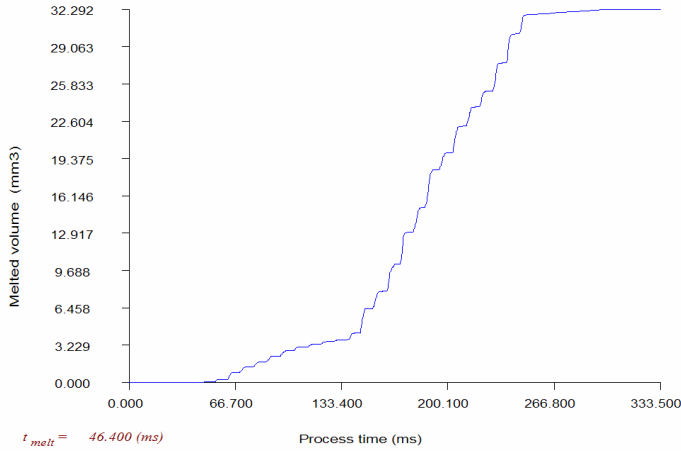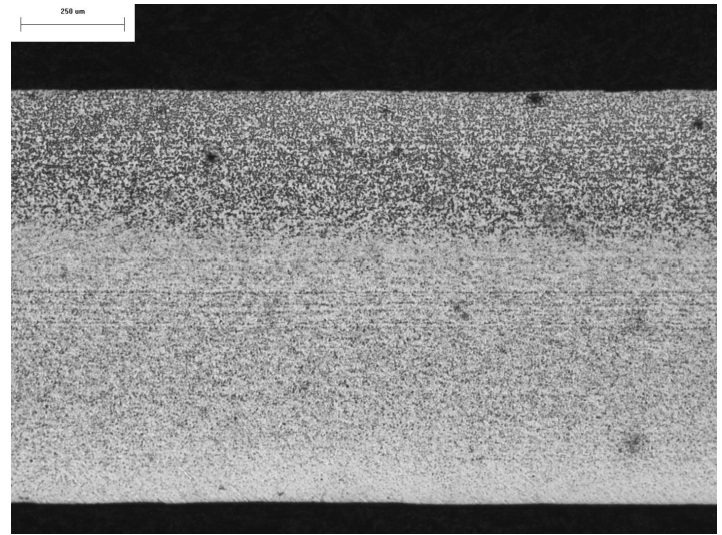| Weld Time		Peel Button Size (nominal diameter, mm)	
		Uncoated Electrode	Coated Electrode
(ms)	cycles		
17	1	0.00	0.00

$t_{melt} = $ 46.400 (ms)

Figure 4: Predicted melted volume of metal for coated electrode weld at 10500A

b)

Figure 5: Uncoated electrode weld sheet after 7 cycles (117ms) of weld current at 10500A. Region A shown in high magnification in b). The top surface is the faying interface.

4 METALLURGICAL STUDY

Cross sectioning of a weld stopped at 7 cycles (117ms) of current using uncoated electrodes is shown in Figure 5. At this point, the weld area showed a slight heat affected zone at the faying interface outlined in a) of the figure. The higher magnification view in b) shows the change in microstructure with no evidence of melting or fusion between the steel sheets. Grain size has increased due to the heating however no solidification structure is evident.

Figure 6 shows the simulated uncoated electrode weld at 150ms (2 cycles of squeeze plus 7cycles of weld). The heating pattern of the figure very closely matches what was seen in the cross section. The solid line at the faying interface represents the molten zinc layer, while the heating profile is clearly present without any melting indicated by the dark solid colour.
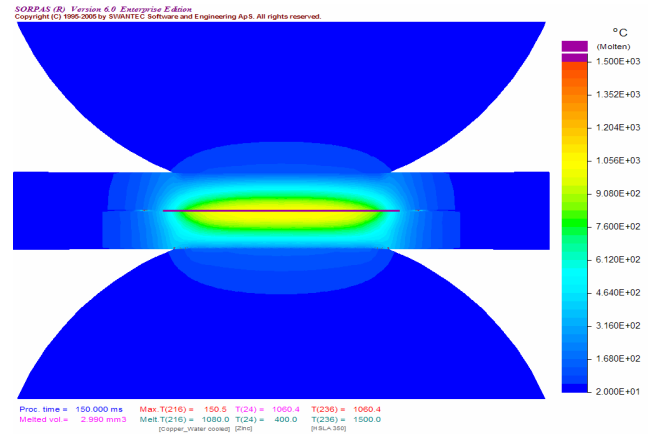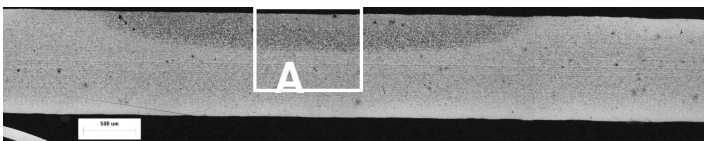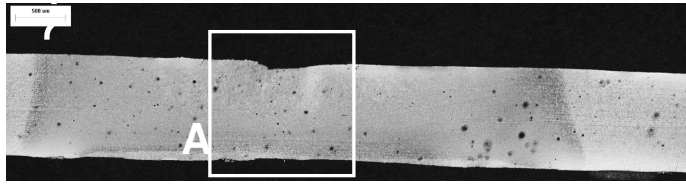

Figure 6: Simulation of uncoated electrode weld at 150ms and 10500A


a)

As shown in Table 4, the uncoated electrode required almost double the weld time to melt the steel at the faying interface. Under the same conditions, the steel sheet welded with the coated electrode is shown in Figure 7. A clear heat affected zone has progressed through the thickness of the sheet and evidence of melting was present at the faying interface. Peel testing had shown that a weld nugget had formed and the sheets had fused and then fractured along the faying interface. Simulation of the weld shown in Figure 8 also suggests that a nugget was formed yet was not large enough to cause a pullout button upon peeling. The higher magnification view in b) clearly shows the solidification microstructure as well as the fracture region. Under similar weld conditions and weld

parameters, the coated electrode was able to produce fusic n where the uncoated electrode was not.


a)
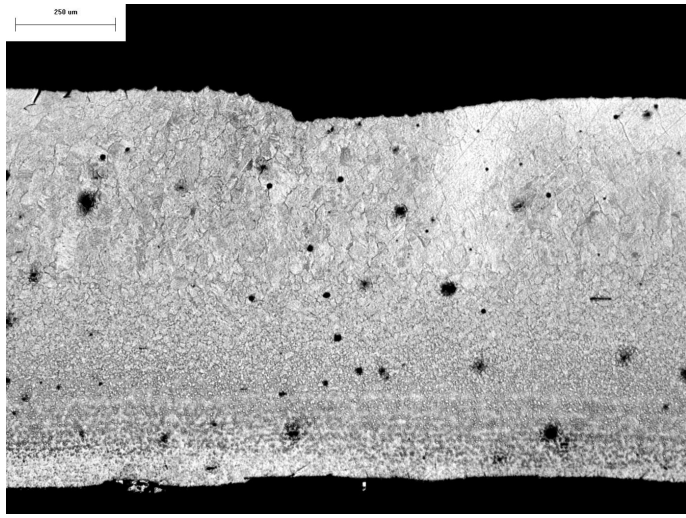
b)

Figure 7:   Coated electrode weld at 7cycles (117ms) of weld current at 10500A. Region A shown in high magnification in b). The top surface is the faying interface.

Figure 8: Simulation of coated electrode weld at 150ms and 10500A

Figure 9 shows the welds at 14 cycles (233ms) of current.   At this point, both coated and uncoated electrodes were able to form welds. The uncoated weld in a) shows the button measured as 4.0mm. The fusion nugget penetration was approximately 30% as shown on the figure.   The coated weld shown in b) displayed a much larger nugget with a measured button of 6.15mm.

The penetration of this nugget was approximately 60%, double that of the uncoated electrode. Again, the coated electrode displayed the ability to produce larger welds under the same welding parameters.

Simulation results for the welds at 14 cycles of weld current are displayed in Figures 10 and 11. Approximate weld sizes for the predicted welds are 4.9mm and 5.55mm for uncoated and coated electrode welds respectively.
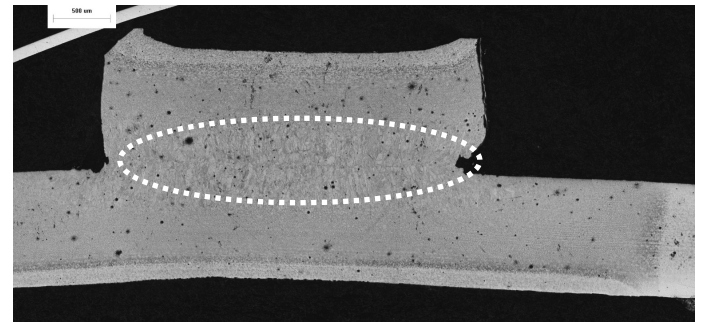
a)
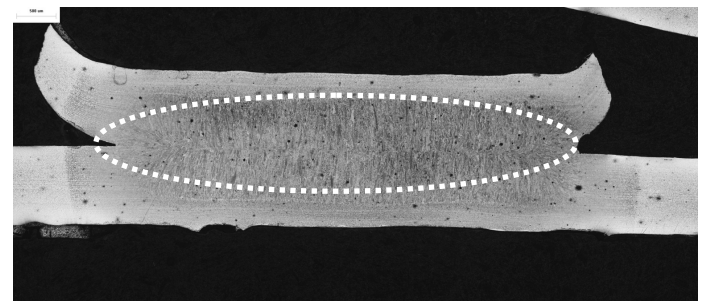
b)

Figure 9: Weld cross sections at 14 cycles (233ms) of weld current after peel testing. a) uncoated, b) coated.
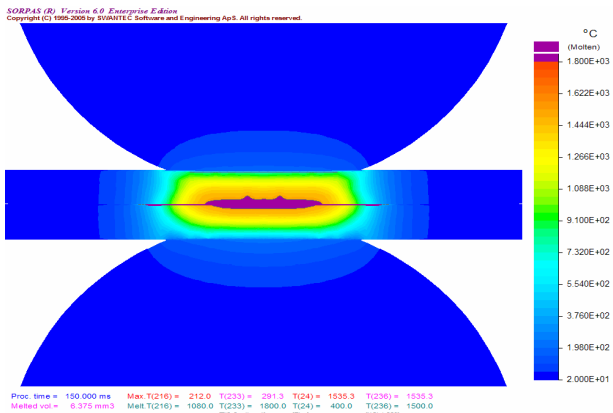

Figure 10: Simulation of uncoated weld at 260ms and 10500A

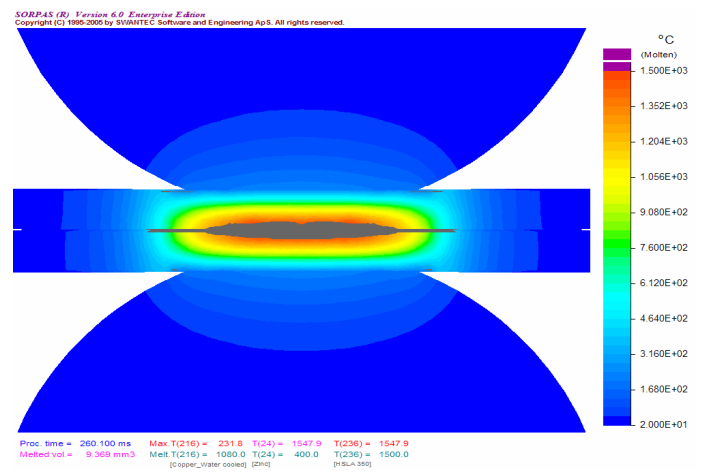Proc. time = 260.100 ms   Max.T(216) = 277.4 T(233) = 347.5 T(24) = 1793.4 T(236) = 1804.5
Melted vol = 31.896 mm3   Melt.T(216) = 1080.0 T(233) = 1800.0 T(24) = 400.0 T(236) = 1500.0
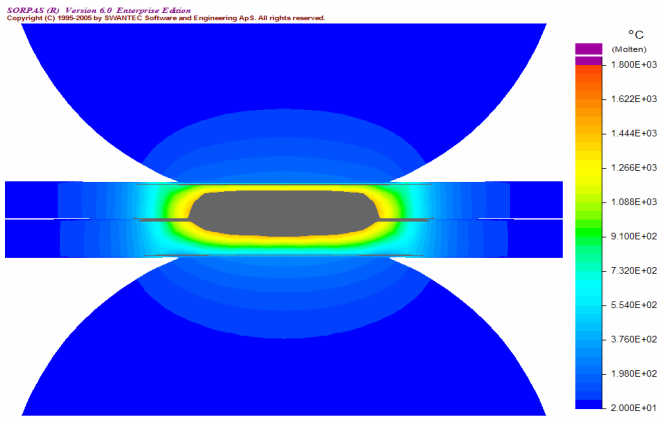[Copper_Water cooled] [TiC Coating -1]   [Zinc]   [HSLA 350]

Figure 11: Simulation of coated weld at 260ms and 10500A

Welding and simulation results consistently indicate that the coated electrode is able to form larger nuggets than the uncoated electrodes under the same welding parameters. The reason for this phenomenon can be due to either an increase in the heat generation or a decrease in the heat lost to the system or a combination of both.

5 ELECTRODE COATING ELECTRICAL RESISTANCE

The presence of a thin layer on the surface of the electrode will affect the resistance of the electrode and could influence the welding behaviour. With the coating-electrode interface added to the system, and a thin film resistance from the coating itself, the RSW system for welding coated steels with coated electrodes has become more complex and is represented schematically in Figure 12.
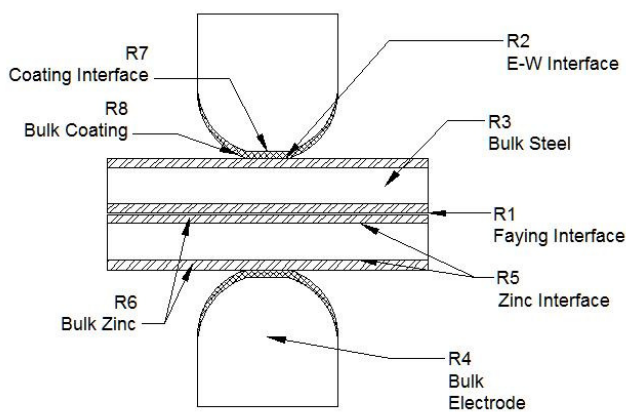

Figure 12:   Coated electrode resistance circuit. R7 and R8 are added to the system due to the electrode coating.

Simulation results were able to calculate the interface resistance at the electrode-work (EW) interface for both uncoated and coated electrodes as shown in Figures 13 and 14.

The EW interface resistance is initially 14μohms and 6.5μohms for coated and uncoated electrodes respectively. As the weld current is applied, both curves show an increase in the interface resistance as expected. The coated electrode resistance reaches a much higher peak at 34.8μohms than the 15.1μohms of the uncoated electrode. The doubling of the resistance with the addition of the electrode coating clearly affects the heat generated at the interface. The resultant increase in the size of the nugget however may not have been due to the increased heat generation alone. The rate of heat extraction from the faying interface is also important in determining the size and shape of the final weld.
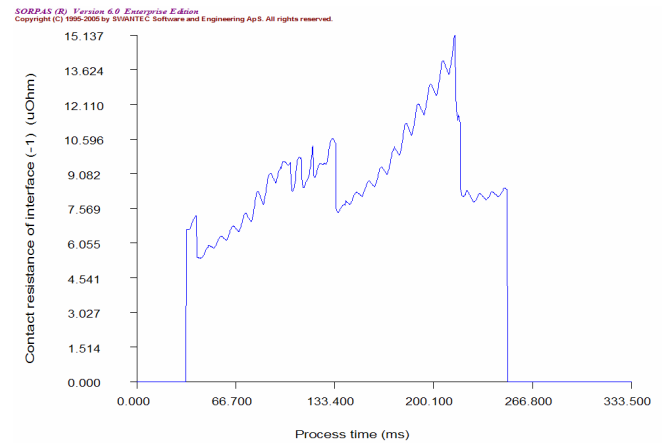

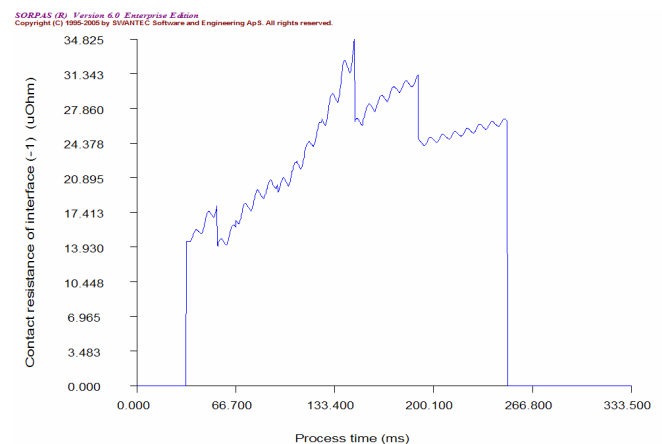Figure 13: EW interface resistance for uncoated electrode weld at 10500A

Figure 14: EW interface resistance for coated electrode weld at 10500A

5.1 ELECTRODE COOLING RATE

Full development of the weld nugget may be restricted by the extraction of heat through the electrodes. Although the resistance at the interfaces has shifted due to the presence of zinc, the thermal gradient across the weld parallel to the electrode axis to the electrode may still be rather small. To approximate the speed of propagation of a transient thermal wave into a body from the surface from which that heat was generated, the basic solution for the standard one-dimensional transient thermal diffusion equation may be of use. Although heat is generated throughout the material and is able to travel in three-dimensions, the simple one-dimensional model can provide insight into the relative speed of a heat wave travelling through the thickness of the sheet. Consider the case of a semi-infinite body initially at temperature T_1 which has one of its surfaces suddenly heated/cooled to a new temperature T_2 at time t = 0. The solution (transient temperature inside the body as a function of time and the distance x from the surface that was heated) is given by [22]:

$$\frac{T - T_2}{T_1 - T_2} = erf\left(\frac{x}{2\sqrt{\alpha t}}\right)$$

where *erf* is the integral of the Gauss curve, and α is thermal diffusivity (m^2/s). Since *erf*(1.0) = 0.84, the position in space-time where $(x/2\sqrt{\alpha t}) = 1.0$ can approximate the front edge of a thermal wave moving through the body. This would mean that the time taken for a thermal wave to propagate through a thickness **x** of a material is of the order of $t = (x^2 / 4\alpha)$. Using thermal diffusivities for Fe and Cu (22.1 and 118 x10^{-6}m^2/s respectively [23]), to approximate that of the RSW system, a transient thermal wave will travel through 0.297 and 0.687mm respectively in 1ms. With weld cycle times on the order of 182ms (11 cycles), it is clear that the thermal gradient across the sheet thickness is very small. This simple model has demonstrated that the heat generated at the faying interface will travel through the entire thickness of the sheets before the weld sequence is over. The effect of heat extraction through the electrodes may become crucial to the formation of the weld nugget.

The propagation of a heat wave generated at the faying interface was able to move very quickly through the material effectively making the thermal gradient in the direction parallel to the electrode axis very small. This makes the rate of heat extraction due to the heat sinking of the electrodes very critical. The presence of molten zinc at the electrode-work interface may also play a role in the thermal circuit of the system. As contact was improved with the liquid zinc layer, the rate of heat transfer to the electrodes would increase. To maximize the efficiency of the RSW process, it is desirable to generate heat at the faying interface as quickly as possible and retain it there, localizing the melting and reducing the negative thermal affects on the workpiece

as well as the weld electrodes. As the thermal diffusivity of copper is more than triple that of iron at room temperature [23], it follows that the electrode will sink a great deal of heat generated reducing the efficiency of the weld sequence. Figures 15 and 16 show the simulated effects of electrode cooling for uncoated and coated electrodes at 250ms into a weld at 10500A. The EW interface in Fig. 15 clearly shows a region of rapid cooling where the electrode is in contact with the worksheets. The interface of the coated weld does not experience this rapid cooling and is thought to result in larger nuggets due to more efficient use of the heat generated.

Close inspection of the heat affected zones of the welds in Figure 9 revealed a thin layer of unaffected base metal very close to the electrode-work interface in the uncoated weld sample. This band of unaffected steel resembled the footprint of the electrode and was evidently due to the heat sinking properties of the uncoated electrode. This distinct band was not present in the coated electrode weld at the same parameters, suggesting that the rate of heat extraction was much lower. Water cooling of the electrodes is necessary to minimize damage to the electrodes caused by excessive heat, but may decrease the efficiency of the weld process by extracting heat needed at the faying interface. The copper electrodes are very good heat sinks and are able to pull heat away from the weld zone quickly. With the lower thermal conductivity coating present at the electrode workpiece interface, another layer was added to the thermodynamic system as well as another interface. Additionally, the small amount of heat generated at this interface due to the increased electrical resistance may also contribute to weld formation. From the discussion above, it has been shown that the coated electrode was able to preserve heat generated in the weld and protects the electrode base material from the same heat.
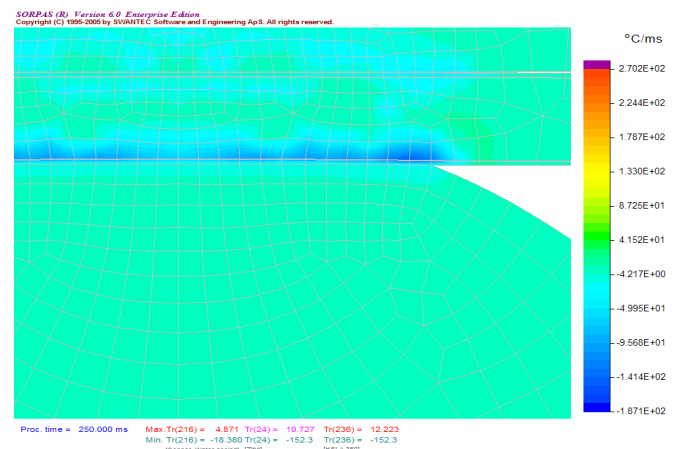

Figure 15: Lower electrode and EW interface cooling rate for uncoated electrode weld at 250ms at 10500A. Rapid cooling is seen at the EW interface.
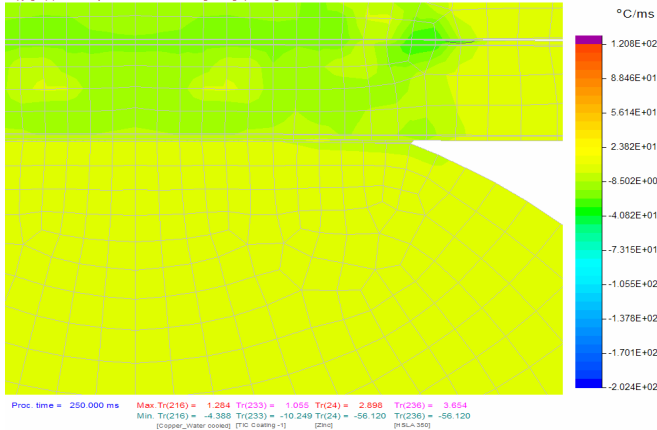
Figure 16: Lower electrode and EW interface cooling rate for coated electrode weld at 250ms at 10500A. Rapid cooling due to the electrode contact is not seen as in the uncoated electrode case.

6 CONCLUSIONS

1. The coated electrode was able to form welds meeting the minimum weld size requirement at lower current and time than the uncoated electrodes. Weldability was increased as seen by a widening and shifting of the current window.
2. Simulation of the resistance spot welding of HDG HSLA steel using both uncoated and coated B-nose electrodes was shown to agree with the laboratory tests. Weld size predictions were shifted somewhat and expulsion was not able to be predicted by the software but could be assumed when a known nugget size is reached.
3. The EW interface resistance of the coated electrode was shown by simulation to be at least twice that of the uncoated electrode. This characteristic is very useful when welding zinc coated steels where the resistances are very low.
4. The cooling rate of the uncoated electrodes was sufficient to cause a cooling artefact in the finished weld. Simulation revealed a very rapid cooling rate at the EW interface of the uncoated electrode. With the electrode coating in place, the rapid cooling was no longer present and the cooling artefact in the weld metal was no longer present.

REFERENCES

1. RWMA Handbook, Fourth Edition, 1989

2. P. Howe, S. C. Kelly, "A Comparison of the Resistance Spot Weldability of Bare, Hot-Dipped, Galvannealed, and Electrogalvanized DQSK Sheet Steels", International Congress and Exposition, Detroit Michigan, February 29-March 4, 1988.

3. J. D. Parker, N. T. Williams, R. J. Holliday, "Mechanisms of electrode degradation when spot welding coated steels", Science and Technology of Welding and Joining, 1998, Vol. 3, No. 2, pp. 65-74

4. R. Holliday, J. D. Parker and N. T. Williams (UK), "Relative contribution of electrode tip growth mechanism in spot welding zinc coated steels", Welding in the World, Vol. 37, No. 4, pp. 186-193, 1996

5. R. Holliday, J. D. Parker and N. T. Williams (UK), "Electrode deformation when spot welding coated steels", Welding in the World, Vol. 35, No. 3, pp. 160-164, 1995.

6. R. Ikeda, K. Yasuda, K. Hashiguchi, T. Okita, T. Yahaba, "Effect of Electrode Configuration on Electrode Life in Resistance Spot Welding of Galvannealed Steel and Aluminum Alloy For Car Body Sheets", IBEC 1995, Advanced Technologies and Proceedings, pp. 144-151

7. T. Saito, Y. Takahashi, T. Nishi, "Electrode Tip Life in Resistance Spot Welding of Zinc and Zinc Alloy Coated Sheet Steels", Nippon Steel Technical Report, No. 37 April 1988, pp. 24-30

8. L. M. Friedman and R. B. McCauley, "Influence of Metallurgical Characteristics on Resistance welding of Galvanized steel", Welding Journal, Supplement, Oct. 1969, pp. 454s-462s

9. Y. Tanaka, M. Sakaguchi, H. Shirasawa, M. Miyahara and S. Nomura, "Electrode Life in resistance spot welding of zinc plated sheets". Int. J. of Materials and Product Tech, vol. 2, no. 1, 1987. pp. 64-74

10. T.V. Natale, " A review of the resistance spot welding behaviour of galvanized steels", Sheet Metal Welding conference III, 1988, Paper No. 1

11. P. Howe, "Resistance Spot Weldability and Electrode Wear Mechanisms of ZnNi EG® Sheet Steel", SAE Technical Paper Series, 910192, 1991.

12. C. T. Lane, C. D. Sorensen, G. B. Hunter, S. A. Gedeon, T. W. Eagar, "Cinematography of Resistance Spot Welding of Galvanized Steel Sheet", Welding Journal, Supplement, September 1987, pp. 260s-265s.

13. R. Holliday, J. D. Parker ad N. T. Williams, "Factors affecting deformation of electrodes when resistance spot welding coated steels", Key Engineering Materials Vols. 99-100 (1995) pp. 95-102

14. S. Dong, Y. Zhou, "Effects of TiC Composite Coating on Electrode Degradation in Microresistance Welding of Nickel-Plated Steel", Metal. And Materials Trans. A., Vol. 34A, July 2003, pp. 1501-1511

15. Huys Industries Limited, < http://www.huysindustries.com/ >, 2004

16. S. A. Gedeon and T. W. Eagar, "Resistance Spot Welding of Galvanized Steel: Part I. Material Variations and Process Modifications", Metallurgical Transactions B, Vol. 17B, Dec. 1986, pp. 879-885.

17. S. A. Gedeon and T. W. Eagar, "Resistance Spot Welding of Galvanized Steel: Part II. Mechanisms of Spot Weld Nugget Formation", Metallurgical Transactions B, Vol. 17B, Dec. 1986, pp. 887-901.

18. S.S. Babu, M. L. Santella, and W. Peterson, "Modeling Resistance Spot Welding Electrode Life". Oak Ridge National Laboratory, 2000

19. M. R. Finlay, "Resistance Spot Welding of Metallic Coated Steels and PVD Coated Electrodes", CRC Australia and WTIA, CRC No. 18, 1996

20. SWANTEC Software and Engineering ApS • Agern Alle 3 • 2970 Hoersholm • Denmark • Phone: +45 4525 4621 • Fax: +45 4593 0190, 2005

21. ANSI/AWS/SAE/D8.9-97, "Recommended practices for test methods for evaluating the resistance spot welding behaviour of automotive sheet steel materials", AWS/SAE, 1997

22. Carslaw H.S., Jaeger J.C., "Conduction of Heat in Solids", Oxford University Press, London, second edition, 1959.

23. Tslaf, A., "Combined Properties of Conductors", Elsevier Scientific Publishing Company, New York, 1981.

24. Chan, K. R., Ding, Y., Unpublished works on TiC electrodes